

Application-specific muscle representations

Victor Ng-Thow-Hing
Fundamental Research Laboratories
Honda R&D Americas, Inc.
vngthowhing@hra.com

Eugene Fiume
Department of Computer Science
University of Toronto
elf@dgp.toronto.edu

Abstract

The need to model muscles means different things to artistic and technical practitioners. Three different muscle representations are presented and the motivations behind their design are discussed. Each representation allows unique capabilities and operations to be performed on the model, yet the underlying mathematical foundation is the same for all. This is achieved by developing a data-fitting pipeline that allows samples that are generated from different data sources to be used in the guided construction of a B-spline solid. We show how B-spline solids can be used to create muscles from contour curves extracted out of medical images, digitized fibre sets from dissections of muscle specimens, and profile curves that can be interactively sketched and manipulated by an anatomical modeller.

Key words: Anatomical modelling, muscles, data-fitting, B-spline solid

1 Introduction

The concept of modelling muscles means different things to different communities. When modelling humans and other animals for use in film animation, the intention is to emulate the effects of superficial muscle anatomy that can be seen to contract and stretch through the skin. For biomechanists, the functional aspects of muscle have greater importance. Muscle models are developed based on controlled experiments with real muscle specimens to create parameterized models that relate generated force with muscle length, velocity of shortening, and neural activation. Simulations use these muscle models as actuators to exert forces on mechanical skeletons to study and reproduce motor tasks. At the structural level, anatomists seek to discover the internal fibre arrangements of muscle and how this *muscle architecture* determines the functional role the muscle plays in the overall context of the body's locomotion system.

The development of muscle models has progressed relatively independently in the animation and biomechanics industries. Justifiably, the trend has been to only model what is needed and to avoid unnecessary complexity. An-

imation applications stress the need for body physiques to appear adequately realistic while biomechanical applications only model the functional aspects of muscle, such as muscle force generation.

Of the many modelling primitives available for such representations, parametric solid representations are particularly convenient. Previously, the B-spline solid model has been used to demonstrate that a large variety of muscle shapes can be compactly represented by a model based on B-spline basis functions[7]. The model's volumetric properties allows internal structures to be specified and scalar field functions to be defined over the entire solid's domain. A data-fitting pipeline has been described that allows deformable muscle models to be built from medical images of transverse slices of muscle anatomy[6]. In this work, the same mathematical framework is used to create entirely different muscle representations that each enable new visualizations and phenomena to be depicted.

The purpose of this work is to demonstrate how considerations of application and user interface drive the development of very different muscle models and that this design process is essential to the success of the model's utility. The next section reviews the previous work in muscle modelling in the fields of animation and biomechanics. In Section 3, the data-fitting pipeline for B-spline solids is reviewed, followed by separate sections for each of the three models developed with their unique applications. We conclude with discussion of current and future applications of these models.

2 Previous work

The idea of anatomical models for human and animal construction was introduced to the computer graphics community using geometric primitives such as ellipsoids, and parametric surfaces[14, 15, 12]. The emphasis on these models was the modelling of general approximations of anatomic muscle groups. As these muscles would never be directly seen because of an obscuring skin surface, there is no need to correctly model exact muscle shapes. Indeed, since the introduction of these methods, many film production houses have implemented

their own proprietary systems to incorporate an anatomical layer of muscles in the modelling pipeline of digital characters[11, 13]. In these applications, secondary dynamic phenomena such as muscle “jiggles” are added to simulate inertial effects. The muscles themselves are used for shape definition and have no functional role in the creation of the motions. Shape changes are mainly driven by joint motion of an underlying kinematic skeleton.

In biomechanics, the venerable Hill model[16] is used ubiquitously to describe force magnitudes of muscle as a function of various parameters such as muscle length, activation and rest length. In combination with a musculo-skeletal system that represents muscle lines of action as piecewise line segment actuators on the skeleton[4], simulations have been made with muscles as active actuators driving tasks such as jumping and walking[9]. As the emphasis is on the functional role of muscle, the volumetric representation of muscle is ignored. Assumptions are made that simplify muscle architecture and inter-muscular interactions that may lead to inaccuracies for some motions. Finite element models that represent both shape and physical function of muscles are usually restricted to single muscles simulated in isolation[3]. The use of the finite-element method generally requires lengthy computational times for detailed simulation that limits the scalability of the technique to large, multiple muscle systems.

One of the goals of using a common mathematical foundation for modelling different muscle representations is the ability to adapt to different levels of complexity using the same set of routines for tasks such as display tessellation and volume calculation. Selective emphasis can be made to focus on graphical, structural, or physical characteristics of muscle contraction.

3 Data-fitting pipeline

The B-spline solid model allows smooth shapes to be defined with a compact set of control point parameters, \mathbf{q} :

$$\mathbf{x}(u, v, w) = \sum_i \sum_j \sum_k B_i^u(u) B_j^v(v) B_k^w(w) \mathbf{q}_{ijk}, \quad (1)$$

where i, j, k index the control point lattice and basis functions of the triple B-spline tensor product. The degree of the basis functions, and thus the resulting solid, can be chosen arbitrarily to meet the smoothness and metric properties demanded by the application. The evaluated points, $\mathbf{x}(u, v, w)$ are the Cartesian coordinates that compose the boundary and volume of the solid being modelled. Given n control points, \mathbf{q} , we can select n material coordinates $\mathbf{u}_i^{max} = (u, v, w)_i, i = 0, \dots, n-1$, that

map to a set of n spatial points, \mathbf{x} :

$$\mathbf{x} = \mathbf{B}(\mathbf{u}^{max})\mathbf{q}. \quad (2)$$

The matrix \mathbf{B} contains the triple tensor products of Equation 1 while the coordinates of \mathbf{u}^{max} are chosen with sampled values of u, v , and w that produce the maxima of each of their corresponding B-spline basis functions. The position of a spatial point, \mathbf{x} , would be most influenced by its corresponding control point, \mathbf{q} , in the same row of Equation 2, providing intuitive control over the solid’s shape as the spatial point is moved.

The data-fitting pipeline requires that spatial points be ultimately provided for each of the known material coordinates, \mathbf{u}^{max} to solve the system in Equation 2. In many cases, the original samples drawn from various muscle sources may not be uniformly distributed. If these data points were directly used as spatial points, the resulting B-spline solid’s control points would be unevenly clustered near the original data. A *continuous volume sampling function* (CVSF) is created from the original data samples of each different muscle representation. A uniform sampling of the CVSF’s domain generates a distribution of spatial points that produces B-spline solids with a uniform arrangement of control points. Furthermore, we can directly solve for any number of control points by generating as many samples as we need from the CVSF.

3.1 CVSF pipeline

The data-fitting process can be described as follows:

1. From various raw data sources, extract 3-D coordinate data that samples the physical object we wish to represent. Samples can occur within the volume of the object as well as on its boundary.
2. Using the 3-D data, construct a *continuous volume sampling function* (CVSF). The CVSF can be described as: $CVSF(\tilde{u}, \tilde{v}, \tilde{w})$, such that $(\tilde{u}, \tilde{v}, \tilde{w}) \in [0, 1]^3$.
3. We uniformly sample the parameter space of the CVSF to generate the same number of spatial points as we have control points in our model. The material coordinates, \mathbf{u}_{max} are assigned to these spatial points.
4. Using the sampled data points as spatial points, \mathbf{x} , solve the linear system described in Equation 2.

Once the B-spline solid is created with an initial shape based on the data points, we can subsequently manipulate the shape or animate global changes through physically-based modelling or deformation.

Of the four stages in the CVSF data-fitting schema, Stages 3 and 4 are independent of the original form of the data. Stages 1 and 2, however, must be designed to accommodate each new muscle representation and application. Equations 1 and 2 provide extremely general ways in which to effect this. While this level of generality is needed to accommodate the different forms of input that different muscle modelling applications may need, there is a clear structure in the way that each application both gathers and represents discrete data. That structure defines a specific traversal of an otherwise very complex volume as well as having semantic importance to the application. We have isolated three structures: contour curves, fibre sets, and profile curves. In the next three sections, we demonstrate how each can be used both to define a novel muscle representation and to accommodate the forms of data sources that are available in that application.

4 Contour curves

Medical imagery containing transverse anatomical cross-sectional slices can be used to perform reconstruction of muscles. For example, portions of the Visible Human data-set[8] in the lower leg region can be used to isolate the boundary form of muscles (Figure 8). Full details of this process are described in [7]. Once muscles have been successfully segmented from the image slices, they can be selectively displayed and examined in relation to neighbouring anatomy.

4.1 Creating the CVSF

Given a set of n contour curves extracted from the transverse slices: C_0, \dots, C_{n-1} , we wish to design a CVSF that produces a uniform sampling of points throughout the volume spanned by these image contour curves. The contour curves are represented as B-spline curves created by interpolating sample points taken along muscle cross-sectional boundaries. The sample points are re-indexed to minimize the distance between corresponding samples on adjacent slices sharing the same index. This step will reduce rotational distortions in the B-spline solid. The CVSF is designed to interpolate the contour curves such that traversing the parameters will span the solid in an intuitive manner. We select parameter \tilde{u} to increase radially outward from a central axis of the solid to its contour boundaries. Parameter \tilde{v} will traverse the perimeter around the axis and \tilde{w} will range from the bottom of the stack to the top (Figure 1).

A curve, $\mathbf{axis}(\tilde{w})$, $\tilde{w} \in [0, 1]$ through the centroids of the contours is defined to travel along the length of the muscle. Given a specific set of parameters, $(\tilde{u}_0, \tilde{v}_0, \tilde{w}_0)$, a second B-spline curve, $\mathbf{profile}_{\tilde{v}_0}(\tilde{w})$ is created on the outer boundary of the muscle that interpolates all of the

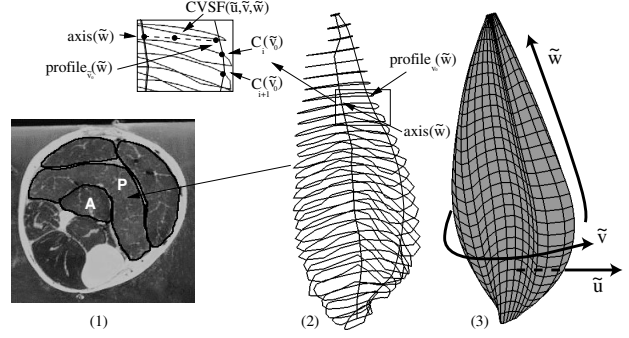


Figure 1: CVSF construction from contour curves

points $C_i(\tilde{v}_0), i = 0, \dots, n - 1$ from each contour. The \tilde{w}_0 parameter generates two points, $\mathbf{axis}(\tilde{w}_0)$ and $\mathbf{profile}_{\tilde{v}_0}(\tilde{w}_0)$, along the length of each of the two curves and these points are linearly interpolated by \tilde{u}_0 to produce the final spatial point.

Using an arclength parameterization for $\mathbf{axis}(\tilde{w}_0)$ and $\mathbf{profile}_{\tilde{v}_0}(\tilde{w}_0)$ ensures that the iso-parametric curves in the \tilde{w} direction of the solid do not undergo excessive twisting and iso-parametric curves in the \tilde{v} around the muscle's axis are evenly distributed along the muscle's length instead of being aligned with the original image slices. Degree 2 B-spline basis functions were used in the v and w domains to reduce unwanted oscillations in the surface yet still produce smooth surfaces. A degree 1 B-spline basis was used for the parameter u to model an even distribution of material from the inner axis to the boundary of the muscles.

By transforming the original static images from the Visible Human data-set to a deformable B-spline solid model, we have animated its shape to simulate contractions[6] and generated muscle fibres as streamlines in the solid's volume. Unfortunately, from an anatomical standpoint, the fibres reconstructed from a B-spline solid derived from medical images do not match muscle architecture observed in real muscle (Figure 2). The contour curves inherently contain only boundary information, losing all internal muscle architectural information. This restricts the use of muscles obtained in this manner to only external muscle visualizations, volume and mass computation, or modelling of general anatomical shapes of muscle groups. It is extremely difficult if not impossible to track individual fibres between adjacent transverse sections. As muscle contracts in the direction of its fibre arrangement, correct modelling of shape changes during muscle activation cannot be obtained for muscles reconstructed from only its boundary surface.



Figure 2: Comparison of generated fibres for the posterior soleus region from different data sources. The image on the left shows fibres incorrectly running from top to bottom in a side view of posterior soleus derived from contour stacks. The right image shows the correct fibre arrangement in a solid generated from fibres obtained by serial dissections.

5 Fibre sets

In order to depict the correct arrangement of fibres that make up muscle tissue, we digitized fibre positions from serial dissections of cadaveric muscle specimens.

5.1 Specimen preparation for serial dissection

The human soleus muscle has three architecturally, distinct regions: posterior, marginal and anterior (Figure 3). In serial dissection, the layers of muscle tissue are removed one at a time from the most superficial layers to the deeper, interior ones (Figure 5). At each layer, representative fibres are selected and digitized to obtain fibre arrangements throughout the entire volume of the muscle as shown in Figure 4. In contrast to previous muscle fibre reconstructions using B-spline solids [6], we have designed a CVSF that incorporates all available fibre data throughout the muscle volume instead of a limited subset of fibres located only on the boundaries of the muscle. This increases the fidelity of the fibre arrangement visualization.

5.2 Fibre set CVSF construction

For each architecturally distinct muscle region, a muscle fibre is represented as a B-spline curve, $\mathbf{fibre}_{i,j}(\tilde{w})$, by interpolating the corresponding digitized 3-D points obtained for each fibre during serial dissection. The index i refers to the layer of muscle the fibre resides in and j indexes the fibres within that layer. The curve is arclength parameterized to ensure spatial points are selected evenly

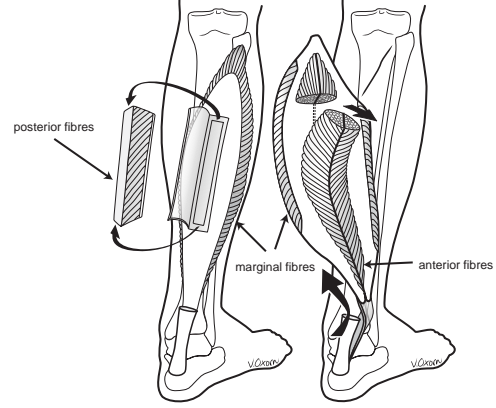


Figure 3: There are three architecturally-distinct regions in the human soleus: marginal, posterior and anterior fibres. Images courtesy of Valerie Oxorn, Copyright 1998-1999.

along the physical length of the fibre. For fibres consisting of two endpoints only, degree 1 B-spline curves are used (i.e., line segments). For all other fibres, degree 2 curves are used. Cubic curves introduced unwanted oscillations with overly long fibre lengths.

The other two parameters, \tilde{u} and \tilde{v} , define the index range that selects four fibre curves to bilinearly interpolate to obtain the final spatial point. Given $(\tilde{u}_0, \tilde{v}_0, \tilde{w}_0)$, we let \tilde{u}_0 travel down through the layers of a muscle and $\mathbf{numLayers}$ be the number of layers obtained with serial dissection. Parameter \tilde{v}_0 travels along the $\mathbf{numFibres}_i$ muscle fibres in layer i . Using floor functions, we compute:

$$\begin{aligned} i &= \lfloor \tilde{u}_0(\mathbf{numLayers} - 1) \rfloor, \\ j &= \lfloor \tilde{v}_0(\mathbf{numFibres}_i - 1) \rfloor. \end{aligned}$$

A bilinear interpolation between the space spanned by the four points,

$$\begin{aligned} \mathbf{p}_{00} &= \mathbf{fibre}_{i,j}(\tilde{w}_0), \\ \mathbf{p}_{01} &= \mathbf{fibre}_{i,j+1}(\tilde{w}_0), \\ \mathbf{p}_{10} &= \mathbf{fibre}_{i+1,j}(\tilde{w}_0), \\ \mathbf{p}_{11} &= \mathbf{fibre}_{i+1,j+1}(\tilde{w}_0), \end{aligned}$$

is performed using the interpolation parameters:

$$\begin{aligned} \hat{u} &= \tilde{u}_0(\mathbf{numLayers} - 1) - i, \\ \hat{v} &= \tilde{v}_0(\mathbf{numFibres}_i - 1) - j \end{aligned}$$

to get the final spatial point with the following steps:

$$\begin{aligned} \mathbf{p}_0 &= \mathbf{p}_{00}(1 - \hat{v}) + \mathbf{p}_{01}\hat{v}, \\ \mathbf{p}_1 &= \mathbf{p}_{10}(1 - \hat{v}) + \mathbf{p}_{11}\hat{v}, \\ \mathbf{CVSF}(\tilde{u}_0, \tilde{v}_0, \tilde{w}_0) &= (1 - \hat{u})\mathbf{p}_0 + \hat{u}\mathbf{p}_1. \end{aligned}$$

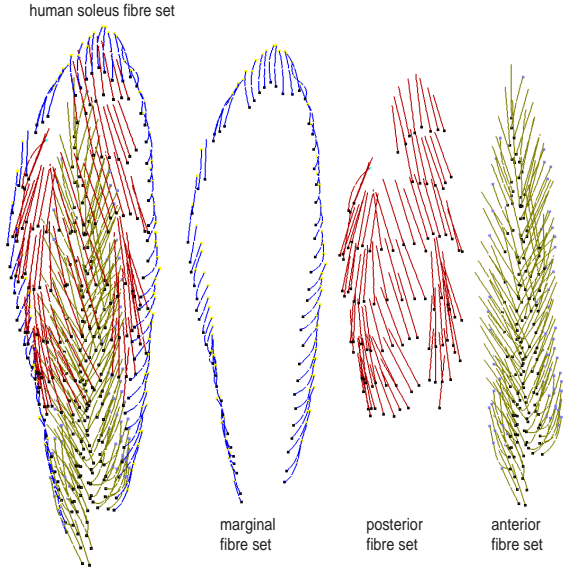


Figure 4: Digitized fibre sets for the three regions of human soleus

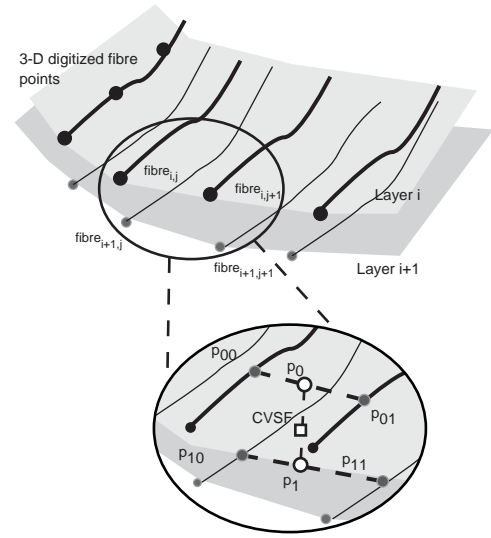


Figure 6: CVSF construction for fibre sets. The CVSF sample point is the result of a bilinear interpolation process on the fibre set data.



Figure 5: Serial dissection of human soleus muscle with marked fibre points

Figure 6 illustrates this process.

With the generated fibres, we can obtain virtual measurements of fibres and their angles of insertion to the tendon region of muscle. These can be used to obtain estimates of muscle force that take into account the finer details of muscle architecture. An arbitrary number of fibres can be visualized within the solid by generating streamlines represented as 3-D space curves. Sampling using parameter values at uniform intervals produces an unnaturally, regular grid-like distribution of fibres. On the other hand, a random sampling of fibres produces uneven clumps of fibres in the muscle. We have found a two-dimensional Sobol sequence[10] guarantees a more even distribution of fibres (Figure 7).

By embedding viscoelastic links with Hill muscle

force models[16], muscle contraction under volume preservation has been simulated (Figure 9). Full details of this process are described in [5]. These fibre set models allow biomechanists to study muscle function to a greater level of detail than previously offered. Cadaver studies on soleus muscle have demonstrated that pennation angles can vary throughout the volume of muscle[1]. Models that account for pennation effects as a single parameter only describe average force production for muscle fibres, losing any information about local regional effects within a muscle. Furthermore, the activation of muscle fibres is not simultaneous. The parameterization of the B-spline solid model permits local fibre regions to be delineated and assigned different activation values. The combination of this ability to model detailed fibre architecture and the provision of a data-fitting pipeline to create models from real specimens makes our model a suitable candidate for extensive functional studies of different muscles.

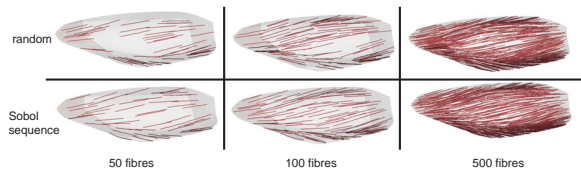


Figure 7: Generation of fibres. 50, 100, and 500 fibres were generated in a model of the posterior soleus using uniform pseudorandom number generation and Sobol sequences. The Sobol sequence produced better distribution of fibres.

6 Profile curves

Contour curves and fibre sets offer a migration path from sources of actual anatomical muscle data to the construction of a virtual B-spline solid model. However, there are occasions where interactive creation of solid shapes is desirable. For example, for an application involving muscle reconstruction of extinct animals, it would be impossible to obtain soft tissue specimens of real anatomy. A computer artist may wish to design a novel creature with a unique musculoskeletal system that does not exist. Generally, a creature designer will use comparative anatomy to guide where major muscle groups are placed on a fictional animal. These applications need to be able to interactively design the shapes of B-spline solids, with visual guidance from a human designer.

In creature modelling applications, the artist needs only approximate shapes of muscle groups because the underlying anatomy will be covered by a layer of skin. Manipulating the individual control points of a B-spline solid would be too tedious. Using multiple *profile curves*, a modeller could capture important features and the overall muscle shape at a higher level of abstraction than through control points.

The attachment of musculotendon onto a skeleton can be characterized by three important curves: *origin*, *insertion* and *axial*. The origin and insertion curves indicate the attachment areas of the tendon portions of a musculotendon to the bony surfaces of the skeleton. The axial curve indicates the direction the muscles takes from one end of the curve to the other - its line of action. If the axial curve connects the centroids of the cross-sections of the muscle, biomechanists can use this curve to calculate the moment arm of the muscle about a joint. Additional curves could be added along the axial curve to further refine the muscle's shape by creating a swept surface of these curves. In our application, a single mid-sectional curve is defined. We have designed a CVSF that constructs the solid muscle using these profile curves (see Figure 10).

The origin and insertion curves are represented as two closed, periodic B-spline curves, **origin**(\tilde{v}) and **insertion**(\tilde{v}). The axial curve is an open, aperiodic B-spline, **axial**(\tilde{w}). We have used degree 2 B-spline curves, but higher order curves can be used. In practice, quadratic curves provide a good compromise between smooth curves and reduced oscillations in the curve. We would like the CVSF to have the following properties that guarantee the solid will interpolate the profile curves on

its boundaries:

$$\begin{aligned} CVSF(1, \tilde{v}, 0) &= \mathbf{origin}(\tilde{v}), \\ CVSF(1, \tilde{v}, 1) &= \mathbf{insertion}(\tilde{v}), \\ CVSF(0, \tilde{v}, \tilde{w}) &= \mathbf{axial}(\tilde{w}), \forall \tilde{v} \in [0, 1]. \end{aligned}$$

The mid-sectional curve, **middle**(\tilde{v}), is generated automatically by averaging the local coordinates of the insertion and origin curves (see Section 6.1 for the calculation of local frames of reference for each curve) and can be initially positioned anywhere along the axis. We chose the halfway point on the axial curve for a balanced weighting between the two end curves. The mid-sectional curve along with the end curves influence the shape of the musculotendon along its length. Rather than linearly interpolating between the sections directly, a nonlinear weighting is made to account for the observation that the shape does not uniformly change from the midsection to the extremal sections. Each cross-section of the solid is desired to be approximately oriented perpendicular to the local tangent of the axial curve.

6.1 Reference frames for the axial curve

To generate points that deform as the axial curve moves, we need to define a local reference frame that can be centred on any \tilde{w} of **axial**(\tilde{w}). We use Bloomenthal's rotation minimizing frame[2] to avoid sudden large changes in orientation of the local frames along the axial space curve. This reference frame can be represented as a 3×3 matrix, $L_{rotmin, \tilde{w}}$ with the origin located at the point, **axial**(\tilde{w}). Having developed a local coordinate system for these profile curves, we will describe an interactive user interface to allow an artist to directly sketch and deform muscle shapes on a skeleton.

6.2 Profile curve sketching with direct manipulation

The user sketches 3-D muscles by selecting points directly on the visible bone surface geometry through which profile curves should interpolate, allowing direct manipulation and editing of points. A musculotendon shape designer would proceed to select points to sketch out the curves for the origin, insertion and axial profiles of the muscle (Figure 10). If the user is using a 2-D pointing device to pick points on an image of a 3-D skeleton, the problem is to find the corresponding 3-D points of the picked geometry.

One alternative is to locate the intersection of a projected ray from the picked screen coordinate with the surface geometry. The computational expense involved in locating the geometric intersection point of this ray in a complex scene may be too high for interactive applications. Furthermore, the original picked point is at pixel

precision, which is already a discrete approximation of the true point on the viewing plane.

Instead, taking advantage of current depth buffer-based graphics hardware, the screen coordinates (x, y, z) are extracted, where x and y are image coordinates and $z \in [0, 1]$ contains the depth buffer value for that pixel. With these coordinates, inverse transformations of the modelling, camera and projection matrices are performed to determine in real-time the corresponding world coordinates for the picked point on the screen.

As we are dealing with discretized representations of the geometry, there is always the danger of imprecision. To minimize this potential inaccuracy, we closely bound the geometry with the near and far clipping planes to increase the dynamic range of the depth buffer. Current depth buffers have 16 to 32 bits of precision, providing enough significant digits for finding adequate world coordinates. A nice side-effect of using this method is that if more precision is required, the designer can zoom the camera closer to the bone geometry, so that accuracy is bound to the discretization error of the picked visible pixel.

6.3 CVSF construction

Having created a local reference frame for our axial curve and having obtained point samples for the origin, insertion and mid-section curves, we now describe how to compute spatial points from these profile curves given the sampling parameters $(\tilde{u}_0, \tilde{v}_0, \tilde{w}_0)$.

The interpolating curves, **origin** (\tilde{v}) , **insertion** (\tilde{v}) , and **middle** (\tilde{v}) are created from point samples obtained interactively from the user. We evaluate the points:

$$\begin{aligned} \mathbf{p}_O &= \mathbf{origin}(\tilde{v}_0), \\ \mathbf{p}_I &= \mathbf{insertion}(\tilde{v}_0), \\ \mathbf{p}_m &= \mathbf{middle}(\tilde{v}_0). \end{aligned}$$

and express them in terms of the axial local frame of references, $L_{rotmin,0}$, $L_{rotmin,1}$, and $L_{rotmin,0.5}$ respectively, to get:

$$\begin{aligned} \mathbf{p}'_O &= \mathbf{p}_O L_{rotmin,0}^T \\ \mathbf{p}'_I &= \mathbf{p}_I L_{rotmin,1}^T \\ \mathbf{p}'_m &= \mathbf{p}_m L_{rotmin,0.5}^T. \end{aligned}$$

The parameter \tilde{w} is used to determine a point, \mathbf{p}' on the muscle's surface through interpolation of the points in Equation 3. Although we can use linear interpolation to get a point, \mathbf{p}' on the muscle's surface, the resulting swept surfaces are not satisfactory and there is only C^0 continuity on the mid-section curve. Rather, we nonlinearly bias the swept surfaces towards the mid-section curve by using a quadratic function. This creates a wider region

of influence in the middle of the muscle that follows the shape of **middle** (\tilde{v}) before tapering off to the origin and insertion curves. Depth in the muscle from the surface to the axis is controlled by scaling the point \mathbf{p}' by \tilde{u}_0 before transforming \mathbf{p}' back to its position in world coordinates:

$$CVSF(\tilde{u}_0, \tilde{v}_0, \tilde{w}_0) = \mathbf{axial}(\tilde{w}_0) + \tilde{u}_0 L_{rotmin,\tilde{w}_0} \mathbf{p}'. \quad (3)$$

By allowing a muscle shape designer to interactively modify the origin, insertion and axial curves, we can completely specify a new B-spline solid which interpolates these profile curves. This technique allows a larger number of control points of the solid to be completely specified by a smaller set of points that make up the curve. Profile curves can be considered a deformation technique to define solid shapes because the points of the solid are referenced and transformed relative to a local coordinate system based on the profile curves. The technique of modelling from profile curves is suitable for high-level design of musculature on a human or animal model as seen in Figure 11, but lacks the fine muscle architectural detail needed for accurate muscle simulations.

7 Conclusion

The development of a consistent framework for data-fitting of B-spline solids allows the flexibility of designing volumetric geometric representations that are tailored to different available data sources. In all cases, careful consideration of how the model will be used plays a major role in the construction of its CVSF. The three applications we presented range from detailed muscle architectural studies to intuitive profile curves for interactive sketching of muscles onto a skeleton. The variety of muscle representations displayed attests to the versatility of the B-spline solid model. However, a significant shortcoming of using B-spline solids is the inability to inherently model branching structures. Although it is possible to create a branched muscle through a union of several B-spline solid muscles, subdivision solids may provide a more elegant method to inherently support branching.

The various muscle models presented here can also be combined to take advantage of the strength of each model's representation. For example, multiple fibre-set muscles can be nested within a single muscle derived from contour curves to visualize intricate fibre arrangements within the boundaries of a muscle extracted from medical imagery. The control points of the enveloping solid can be used directly as a free-form deformation, ensuring the nested solids deform with the solid that contains them. A unified B-spline solid framework can be used to construct a digital library of muscle models containing various levels of detail from general muscle

groups to detailed muscle fibre arrangements.

Acknowledgements

We would like to thank Anne Agur and Nancy McKee from the University of Toronto's Department of Anatomy for motivating the need to model accurate muscle fibre architecture and for performing the data collection of muscle fibres from cadaveric specimens. We thank Honda R&D Americas for their continued support of this work and the anonymous paper reviewers for their useful suggestions and comments.

References

- [1] A.M.R. Agur and N.H. McKee. Soleus muscle: Fiber orientation. *Clinical Anatomy*, 10:130, 1997. Abstract.
- [2] J. Bloomenthal. Calculation of reference frames along a space curve. In Andrew S. Glassner, editor, *Graphics Gems*, pages 567–571. Academic Press, Inc., 1990.
- [3] D. T. Chen and D. Zeltzer. Pump it up: Computer animation of a biomechanically based model of muscle using the finite element method. In *Computer Graphics (SIGGRAPH '92 Proceedings)*, volume 26, pages 89–98, July 1992.
- [4] S. L. Delp, J. P. Loan, M. G. Hoy, F. E. Zajac, E. L. Topp, and J. M. Rosen. An interactive graphics-based model of the lower extremity to study orthopaedic surgical procedures. *IEEE Transactions on Biomedical Engineering*, 37(8):757–767, 1990.
- [5] V. Ng-Thow-Hing. *Anatomically-based models for physical and geometric reconstruction of humans and other animals*. PhD thesis, University of Toronto, 2001.
- [6] V. Ng-Thow-Hing, A. Agur, K. Ball, E. Fiume, and N. McKee. Shape reconstruction and subsequent deformation of soleus muscle models using b-spline solid primitives. In S.L. Jacques, editor, *Laser-Tissue Interaction IX, SPIE proceedings 3254*, pages 423–434, 1998.
- [7] V. Ng-Thow-Hing and E. Fiume. Interactive display and animation of b-spline solids as muscle shape primitives. In *Computer Animation and Simulation '97*, pages 81–97. Springer-Verlag/Wien, 1997.
- [8] U.S. National Library of Medicine. The visible human project. MRI, CT, and axial anatomical images of human body, October 1996.
- [9] M. G. Pandy and F. C. Anderson. Three-dimensional computer simulation of jumping and walking using the same model. In *VIIth International Symposium on Computer Simulation in Biomechanics*, pages 92–95, 1999.
- [10] William H. Press, Saul A. Teukolsky, William T. Vetterling, and Brian P. Flannery. *Numerical Recipes in C*. Cambridge University Press, second edition, 1992.
- [11] H. Rijkema and B. J. Green. Skinning cats and dogs using muscle deformations. In *Siggraph 2001 Conference abstracts and applications*, page 262, 2001.
- [12] F. Scheepers, R. E. Parent, W. Carlson, and Stephen F. May. Anatomy-based modeling of the human musculature. In *Computer Graphics (SIGGRAPH '97 Proceedings)*, pages 163–172, August 1997.
- [13] D. Turner and S. Marino. Dynamic flesh and muscle simulation: Jurassic park iii. In *Siggraph 2001 Conference Abstracts and Applications*, page 173, 2001.
- [14] J. Wilhelms. Animals with anatomy. *IEEE Computer Graphics and Applications*, 17(3):22–30, 1997.
- [15] J. Wilhelms and A. Van Gelder. Anatomically based modeling. In *Computer Graphics (SIGGRAPH '97 Proceedings)*, pages 173–180, August 1997.
- [16] F. E. Zajac. Muscle and tendon: Properties, models, scaling, and application to biomechanics and motor control. *Critical Reviews in Biomedical Engineering*, 17(4):359–411, 1989.

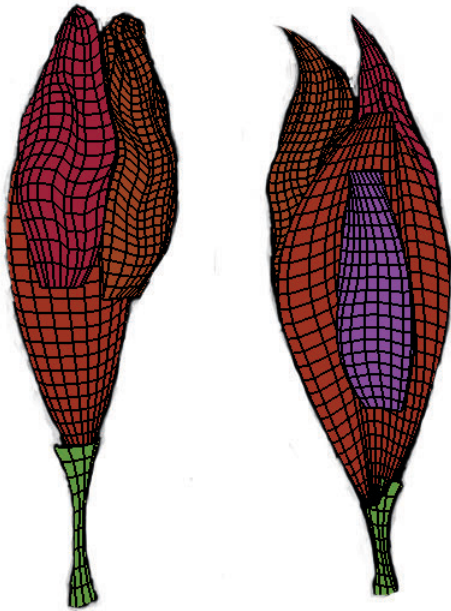


Figure 8: Soleus and gastrocnemius muscle reconstructed from Visible Human data

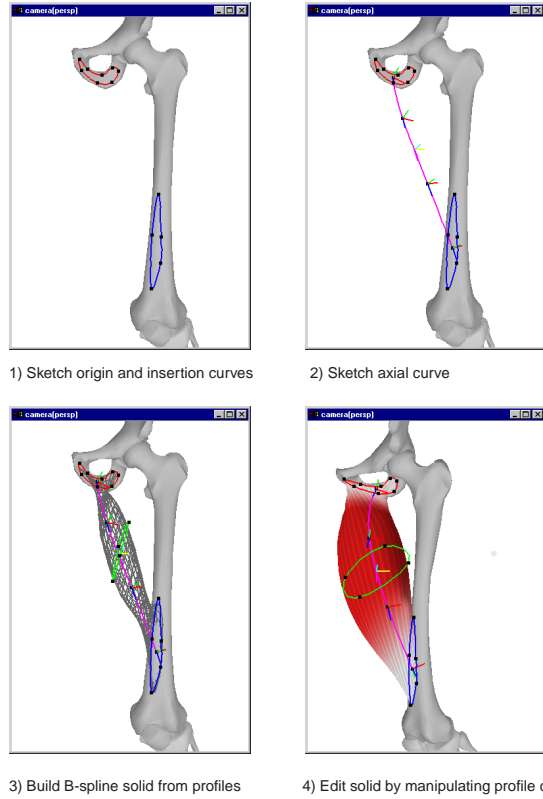


Figure 10: Stages of development of B-spline solids from profile curves. The middle curve is generated automatically in step 3. In the fourth step, the solids can be shaded and textured with striation patterns.

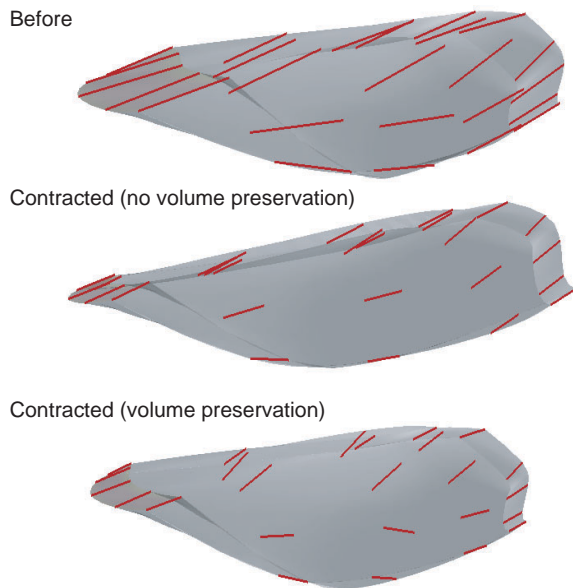


Figure 9: Detailed simulations of muscle contraction can be performed on muscles derived from fibre sets.

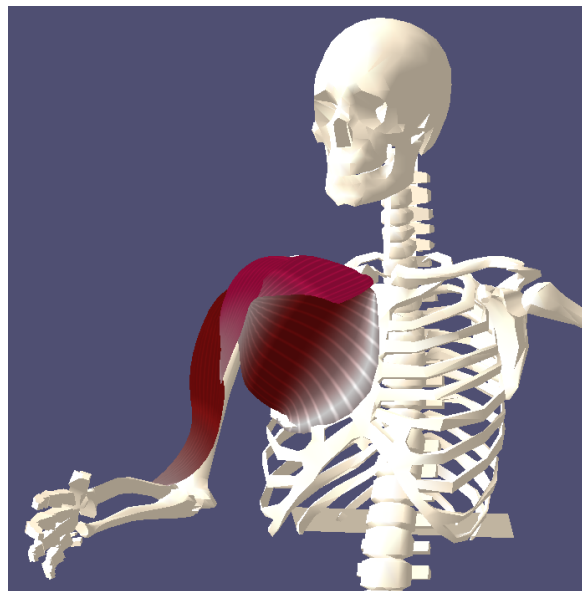


Figure 11: Anatomy-based modeller using profile curves to sketch muscles on a skeleton